Axial distribution of difference frequency sound in a collimated beam of circular cross section.

H. Hobæk and M. Vestrheim
Dep. of Physics, University of Bergen, Norway.

I. Introduction.

Although the far field of the sound generated by non-linear interaction of soundwaves in a beam has received the greatest interest, there have also appeared some papers reporting on observations within the near field, especially along the axis.[1-4] It has been shown[1] that the distribution of difference frequency sound differs markedly from the distribution calculated for infinite plane waves[5,6], and also that it depends strongly on the beamradius and the intensity of the primary waves. In this paper these effects will be considered in more detail. We shall employ a model of plane but collimated primary waves, and later try to account for the effect of nonlinear attenuation of the primary waves. At first, however, we shall examine the validity of using plane collimated primary waves as an approximation to the real near field of the primary waves, when these are radiated from a circular piston.

II. The near field of the primary waves.

A general discussion of the acoustical near field of a circular piston, based upon analytical and numerical solutions, is presented in Ref.(7). For the purpose of discussing the influence of the near field on non-linear interaction some of the conclusions from Ref.(7) are presented in the Appendix. The results are presented in terms of the non-dimensional distance $Z=(x/a)(1/N)$ where x= axial distance, a= source radius and $N=a/\lambda$, λ= wavelength. The transverse distance σ is scaled in a: $b=\sigma/a$. We shall limit discussion to the case where interaction chiefly takes place inside the near field, i.e.

$(\alpha_a+\alpha_b)^{-1} < a^2/2\lambda$, $\alpha_{a,b}$ = attenuation coefficients of the primary waves.

Perhaps the most important property of the beam in this connection is that the phase is virtually constant across the beam, since the maximum phase-difference between points on a cross section will be of order $\pi/8$. This means that if two different waves are present the maximum phase shift between the virtual sources on a cross section will not surmount $\pi/4$. Also, since the phase angles recede quite rapidly for $\sigma>a$, accompanied by a rapid reduction of the amplitude, the interaction region will virtually be confined to a cylinder with radius the same as the source. The effect of the paraxial region will be of minor importance since it occupies only a small portion of the cross section area.

The intensity is not uniformly distributed within the beam. Since the strength of the virtual sources will be proportional to the product of the primary wave amplitudes one may roughly assume that the greatest contribution to the generated sound will come from the region defined somewhat arbitrarily by the lateral extension of the plateau of amplitude 1. The latter shrinks to some 70% of the source radius at $Z\approx0.5$, whereafter the distinction of a plateau ceases to have any significance. This beam contraction does not increase the intensity, which shows that the rest of the energy is radiated away by the sidelobes. It is well known that the main lobe, which is the continuation of the plateau region in the far field, contains almost 84% of the total energy. Thus, when amplitudes alone are considered, one should expect the generated sound to reach an amplitude not less than 84% of the amplitude attainable from an ideal beam of plane collimated waves. In this estimate the effects of the amplitude fluctuations within the beam are ignored. These are difficult to account for, but since the two primary fields will differ in structure it seems fair to regard these effects as of minor importance. The effect of the beam contraction may be significant in the directivity pattern of the generated sound, which should become broader with decreasing beam radius. It could also show an effect in the axial distribution, making the distance from the

source to the major maximum smaller.

One should also be aware that non-linear attenuation will not affect the primary beam in the same way as the linear attenuation. The latter turns out to leave the beam structure virtually unchanged, while the non-linear attenuation will affect the regions of higher amplitude much more than those of low amplitude. One should expect then that this should tend to smooth the field within the primary beam.

In view of this discussion the model of plane collimated primary waves should not be too far-fetched, and we know -to some extent at least- how deviations may occur when comparisons are made to a real beam.

III. Basic equations.

We shall employ the equation obtained in Ref.(6) which describes the generation of difference frequency sound by interaction of two primary waves in a dissipative fluid correctly up to -and including- terms of order M_1^2 and $M_1 S_1$ relative to ambient values, where M and S denote Mach- and (modified) Stokes-number respectively:

$$M = \frac{|\rho - \rho_o|}{\rho_o} \quad , \quad S = 2\alpha/k \quad . \tag{1}$$

Here ρ= density of the fluid, $k = \omega/c$, c = velocity of sound, $\omega = 2\pi f$ where f = frequency, and α= (linear) attenuation coefficient. Here and later, numerical suffixes refer to the order of perturbation: o,1 and 2 denoting ambient, first and second order quantities respectively, while a and b denote the primary frequencies and -,+,2a and 2b refer to the different frequency components. The equation for the generated difference frequency sound may, after elimination of the time dependance, be expressed as

$$\nabla^2 q + \chi_-^2 q = \frac{A+2}{2} \rho_o c_o^{-2} k_-^2 k_a k_b \Phi_a \Phi_b^* = Q \tag{2}$$

Here $\chi = k - i\alpha$, Φ = space dependant part of the primary velocity potentials and $A = \rho_o c_o^{-2} (d^2P/d\rho^2)_o = B/A$ = non-linearity parameter. An asterisk means complex conjugate. Similar equations may be obtained for the other second order waves. Note that the attenuation term which appears on the left hand side of eq.(2) is of order $M_1^2 S_2$, and should

accordingly have been excluded, but is kept for obvious physical reasons. Only the real part of q contains the wanted information, and even this is composite, consisting of the second order density ρ_- plus a term involving the interaction energy:

$$g = \mathrm{Re}(qe^{i\omega t}) = \rho_- + c_o^{-2}[T_{ab} + (\Lambda-1)V_{ab}] \qquad (3)$$

where $T_{ab} = \frac{1}{2}\rho_o \mathrm{Re}(\underline{v}_a \cdot \underline{v}_b^*)$, $V_{ab} = \frac{1}{2}\rho_o c_o^{-2}\mathrm{Re}(\rho_a \rho_b^*)$,

the interaction kinetic and potential energy density respectively. It is easy to show, for instance from the infinite plane wave solution,[6] that the interaction energy term is negligible in most cases, except very close to the source (a few wavelengths). In the next section the solution of eq. (2) will be sought by the use of Greens method after having the boundary conditions specified.

IV. Axial distribution in a collimated beam.

The primary waves are now supposed to be plane and confined to a cylindrical beam of radius a, and we are seeking an expression for the generated sound on the axis of this beam. The configuration lends itself to the use of cylindrical coordinates (x,σ,Θ), and the integration volume is taken to be the halfspace $x \geq 0$. The symmetry eliminates any dependance on Θ. To separate the observation point from the source points the coordinates of the latter are primed. The boundary conditions on q are taken to be[6] $q(0) = 0$ and $\lim_{x\to\infty} q(x) = 0$. These conditions also apply to the Greens function, of which a suitable form is

$$G(\underline{r}-\underline{r}') = \frac{e^{-ik r_I}}{4\pi r_I} - \frac{e^{-ik r_{II}}}{4\pi r_{II}} \qquad (4)$$

where $r_{I,II} = [(x \pm x')^2 + \sigma^2]^{\frac{1}{2}}$, (+) corresponding to r_{II} and (-) to r_I. r_I is the direct distance from a source point $s(x',\sigma')$ to the observation point $P(x,0)$, while r_{II} represents the same distance reflected in the plane of the primary source. The distribution of the generated sound may now be obtained by

$$q(x) = -2\pi \int_0^\infty dx' \int_0^\infty Q(x',\sigma')\, G(\underline{r}-\underline{r}')\sigma' d\sigma'. \qquad (5)$$

The source density $Q(x',\sigma')$ depends on σ' only in that

it vanishes outside the beam, beeing constant within. When G is subsituted in eq.(5) one finds after integration over σ'

$$q(x) = \frac{1}{2\pi\chi_-}\int_0^\infty \hat{q}(x')\left\{\left(e^{-i\chi_-[(x-x')^2+a^2]^{\frac{1}{2}}} - e^{-i\chi_-|x-x'|}\right)\right.$$
$$\left.-\left(e^{-i\chi_-[(x+x')^2+a^2]^{\frac{1}{2}}} - e^{-i\chi_-(x+x')}\right)\right\} dx'. \qquad (6)$$

This expression is fairly obvious, and might have been stated directly. The first bracket represents the axial field at a distance (x-x') from a circular piston of radius a. This part of the contribution to q is then due to a continous distribution of virtual circular sound-sources along the positive x-axis. The last bracket is its image and represents a distribution along the negative x-axis. Another point of view is to note that the last terms in each bracket together constitute the infinite plane wave solution, while collimation is taken into account by the two first terms. The infinite plane wave solution is well known.[5,6]

The last bracket in eq.(6) gives rise to contributions which must be interpreted as backward-radiation, and so does the first for x'> x. The magnitude of this backward-radiation relative to forward-radiation is easily evaluated in the infinite plane wave case, and one finds

$$\left|\frac{q^b}{q^f}\right| = \left|\frac{\alpha_a+\alpha_b-\alpha_-}{2k_-+i(\alpha_a+\alpha_b-\alpha_-)}\right| = O(\alpha_a/k_-)=O(\tfrac{1}{2}S_a\omega_a/\omega_-). \qquad (7)$$

In our experiment we have $\alpha_a/k_- \approx 10^{-3}$. Whether this backward-radiation is physically existing or just a mathematical concept is not known, but its order of magnitude justifies discardance. With the source density expressed as

$$Q(x) = C\, e^{-ik_-x - (\alpha_a+\alpha_b)x} \qquad (8)$$

where

$$C = \frac{\Lambda+2}{2}\rho_o k_-^2 M_a M_b$$

one then has to solve

$$q(x) = \frac{C}{2\pi\chi_-}\int_0^x e^{-ik_-x'-(\alpha_a+\alpha_b)x'}\left\{e^{-i\chi_-[(x-x')^2+a^2]^{\frac{1}{2}}}\right.$$
$$\left. - e^{-i\chi_-(x-x')}\right\} dx'. \qquad (9)$$

The last part of the integral is elementary while no analytical solution has been found to the first part. For the purpose of numerical integration it is convenient to transform to nondimensional quantities $y=x/a$, $K=ak_-$, $A=a(\alpha_a+\alpha_b)$, and when we neglect α_- in the first exponential in the bracket (a fair assumption when $\alpha_- \ll \alpha_a+\alpha_b$), eq. (9) after some manipulation appears as

$$q(y) = \frac{iaC}{2\gamma_-} e^{-iKy}[E(y)-B(y)] \qquad (10)$$

where

$$E(y) = \frac{e^{-a\alpha_- y} - e^{-Ay}}{A - a\alpha_-} \text{ ,(inf. plane wave solution)}$$

$$B(y) = e^{-Ay-iK}\int_0^y e^{+Az-iK[(z^2+1)^{\frac{1}{2}}-(z+1)]}dz \ .$$

After re-introduction of the time factor and extraction of the real part we obtain the distribution expressible as

$$\rho_-(y,t) = |\rho_-(y)| \sin[\omega t - Ky + \mu(y)] \qquad (11)$$

with

$$|\rho_-(y)| = \frac{A+2}{4} \rho_0 \, ak_- M_a M_b F(y)$$

$$\tan(\mu) = [Re(B)-E]/\ Im(B)$$

$$F(y) = \{[Im(B)]^2 + [E - Re(B)]^2\}^{\frac{1}{2}}$$

Our concern in μ is only to check that $d\mu/dy \ll K$, since only in the complete solution can one expect to find μ = constant. The computational result $(d\mu/dy)/K = O(10^{-3})$ must be considered satisfactory.

Fig. 1 shows results from eq. (11)[6] with the parameters used in our experiment: $a=6.5$ mm, $f_-=1.0$ MHz, $f_a=17.68$ MHz, together with the observed distribution. Evidently the agreement is quite satisfactory, especially when one considers the approximations made in the primary fields. (A slight reduction of the effective radius (5%) makes the agreement even better). The experiment will be discussed in section VI. Do note the peculiar little "hump" in the amplitude at $y=2$. This hump is also observed almost at the right place, but slightly less pronounced, probably due to the finite size of the probe. The hump is found to grow with difference frequency, which is also confirmed by experiments. This hump is in fact only the largest of a series of small fluctuations near the source,

and is intimately connected to the near field of the virtual array, not to the near field of the primary waves. It should be noted that a similar hump may be seen in the axial distribution of 2. harmonics generated in a circular piston beam as observed by Gould et al.[6] In their case, however, the hump occurs near the limit of the primary near field, so that the paraxial region of the latter may play a significant part in determining the structure of the hump.

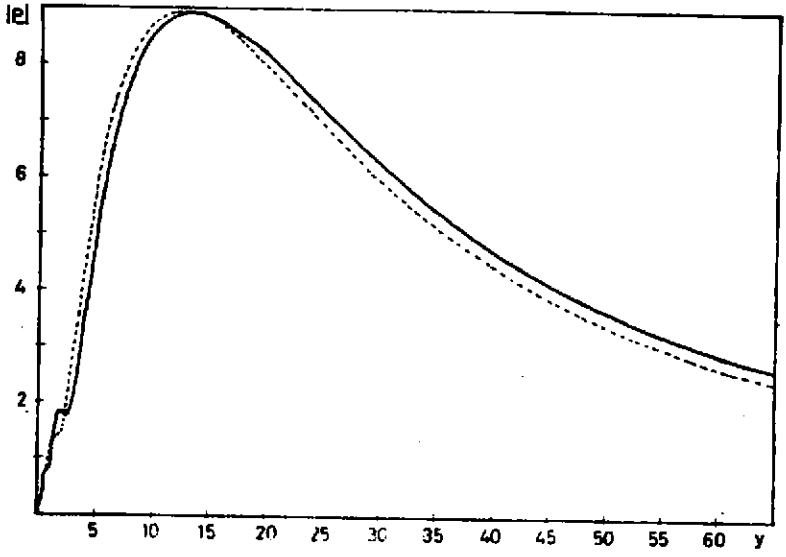

Fig. 1. Axial distribution of difference frequency sound amplitude as computed from eq.(11)[§] : ———, and as observed : ------. The curves have been normalized in amplitude at the maximum. Horizontal axis is axial distance in nondimensional units (y=x/a), vertical is amplitude in arbitrary units.

§) To obtain sufficient resolution from noise over the range of distances shown it was necessary to use primary wave amplitudes corresponding to Re=0.08. A correction for this is incorporated in the theoretical curve in fig.1, as obtained in the next section. The slight effect this has on the theoretical distribution is demonstrated in fig.2.

V. Nonlinear attenuation.

Experimentally it is found that the distribution of the generated difference frequency sound is very sensitive to the amplitudes of the primary waves. The distance to the maximum, y_{max}, for instance, seems to reach its upper limit for primary intensities so small that the generated sound is hardly resolvable from noise ($I_a \approx I_b \approx 10^{-3}$ W/cm^2). The most obvious explanation to this seems to lie in the fact that when successive approximations are used to second order only, the energy is not conserved since the primary waves are quite unaware of their transfer of energy to the new sound waves. This violation of energy conservation is not really important provided the transferred energy represents a vanishing part of the total energy. Thus, the energy transferred to the difference frequency wave does not give reason for any alarm, but this is not so when the second harmonics and the sum frequency waves are concerned.

What we propose to do, of course, is to estimate the amount of energy transferred to these waves, correct for this in the virtual source density as used in the preceeding section, and recalculate the distribution for the difference frequency. This procedure is not quite equivalent to the calculation of the third order approximation of the basic equations, although one should expect the gross result to be the same. Note that since the basic equations are valid only to second order the third approximation would not necessarily yield a better result than the suggested method when the results are compared to experiments.

The second harmonics and the sum frequency will have directivities at least as high as the primary frequencies, and for the purpose of estimating the energy transfer to these waves, it will be sufficient to apply a plane wave approximation. The amplitude of the difference frequency wave in the infinite plane wave case may be written in the form

$$|p_-| = \frac{\Gamma_a}{4} |p_b| \frac{\omega_-}{\omega_b} e^{-\alpha_- x} \left(1 - e^{-2\sqrt{\alpha_a \alpha_b}\ x}\right) \qquad (12)$$

where we have utilized $\alpha=\beta'\omega^2$ (β'=constant) and where

$$\Gamma_a = (A+2)\mathrm{Re}_a = (A+2)\frac{M_a}{S_a} = \frac{1}{\alpha_a L_a} = \frac{A+2}{2}\,\frac{|\rho_a|}{\beta'\omega_a\rho_o c_o} \quad .$$

L_a is the discontinuity distance for the ω_a wave when attenuation is neglected, Re is the acoustical Reynolds number which, as does Γ, serves as a convenient number for describing the relative importance of nonlinearity versus viscosity. Roughly, nonlinearity may be assumed dominant when $\Gamma>1$, i.e. viscosity may then not prevent the formation of a shock-front, and accordingly, harmonics to a high order will be generated.

The sum frequency may be calculated in the infinite plane wave case in an analogous manner[9], as may also the second harmonics, and the result is

$$|\rho_+| = \frac{\Gamma_a}{4}|\rho_b|\frac{\omega_+}{\omega_-}\,e^{-(\alpha_a+\alpha_b)x}\{1 - e^{-2\sqrt{\alpha_a\alpha_b}\,x}\}$$

$$|\rho_{2a}| = \frac{\Gamma_a}{4}|\rho_a|\,e^{-2\alpha_a x}\{1 - e^{-2\alpha_a x}\} \qquad (13)$$

$$|\rho_{2b}| = \frac{\Gamma_a}{4}|\rho_b|\,e^{-2\alpha_b x}\{1 - e^{-2\alpha_b x}\}$$

The same result may be obtained by the use of Burgers equation, see for instance Ref.(10).

If $\omega_a\approx\omega_b$ and $\alpha_a\approx\alpha_b$ the expressions inside the brackets will be nearly equal, and ρ_+, ρ_{2a} and ρ_{2b} will experience almost the same distribution in the x-direction. Note that ρ_+ almost doubles the amplitude of the second harmonics. The ρ_- wave will be distributed differently, and attenuated more slowly. The amplitude will be of order ω_-/ω_b relative to ρ_{2a} and ρ_{2b} (when $\rho_a\approx\rho_b$). Concerning the energy density of the difference frequency wave relative to the other second order waves, one finds

$$\frac{W_-}{W_2} = O\left(\frac{1}{6}\left(\frac{\omega_-}{\omega_b}\right)^2\right) ,$$

which in our experiment amounts to the order of 10^{-4}. Thus, one should be careful in stating the validity of the second order approximation in terms of the magnitude of the difference frequency alone.

To determine how energy is transferred from the primary waves one may employ the Manley-Rowe equations[11], and since the discussion above allows us to neglect the

ρ_- wave, we find that when $\Gamma_a \approx \Gamma_b$ and $\omega_a \approx \omega_b$ the energy-transfer is very nearly equipartioned between the two primary waves. If we then denote by $\langle W_{a1}(x)\rangle$ the time mean of the energy of one primary wave not submitted to nonlinear attenuation and $\langle W_2(x)\rangle$ the energy transferred to the second order waves, we may find the remaining energy density of the primary wave $\langle W_{a2}(x)\rangle$ by applying energy conservation:

$$\langle W_{a1}(x)\rangle\, e^{2\alpha_a x} = \langle W_{a2}(x)\rangle\, e^{2\alpha_a x} + \langle W_2(x)\rangle\, e^{4\alpha_a x}\ , \quad (14)$$

where the exponentials are introduced to compensate for the different attenuations of the first and second order waves. Applying equipartition and $\langle W\rangle \propto |\rho|^2$ we now obtain

$$|\rho_{a2}|^2 \approx |\rho_{a1}|^2\, e^{-2\alpha_a x}\left\{1 - 3\left(\frac{\Gamma_a}{4}\right)^2\left[1 - e^{-2\alpha_a x}\right]^2\right\},$$

i.e. when $\Gamma < 1$ or $\Gamma_a \alpha_a x < 1$ (i.e. $x < L$):

$$|\rho_{a2}| \approx |\rho_{a1}|\, e^{-\alpha_a x}\left\{1 - \frac{3}{2}\left(\frac{\Gamma_a}{4}\right)^2\left[1 - e^{-2\alpha_a x}\right]^2\right\}. \quad (15)$$

This result may be compared to the result of Keck and Beyer[12] who considered distortion of an originally sinusoidal wave of finite amplitude, and solved a basic equation, very similar to the one from which eq.(2) is derived, to high orders. Their third order solution corresponds to

$$|\rho_{a2}| \approx |\rho_{a1}|\, e^{-\alpha_a x}\left\{1 - \tfrac{1}{2}\left(\frac{\Gamma_a}{4}\right)^2\left[1 - e^{-2\alpha_a x}\right]^2\right\}. \quad (16)$$

The same result has been obtained by the use of Burgers equation, see for instance Blackstock[13]. Notice that the production of a sum frequency wave introduces a reduction of the primary wave amplitude which is thrice the effect of the second harmonic alone.

By introducing these corrected expressions for the amplitude of each of the primary waves in the source term in eq.(6) we are now able to obtain an expression for the distribution of the difference frequency sound which involves the parameter Γ for the amplitude of the primary waves, and at least should provide us with a first order approximation to the dependence with the primary amplitude.

The infinite plane wave part of the solution is still easily integrated, and with the introduction of

$$D_{mn} = \frac{e^{-\alpha_- x} - e^{-(m\alpha_a + n\alpha_b)}}{a(m\alpha_a + n\alpha_b - \alpha_-)}$$

it may be expressed as

$$E(x,\Gamma) = D_{11} - 3\left(\frac{\Gamma}{4}\right)^2\left\{D_{11} - [D_{31}+D_{13}] + \tfrac{1}{2}[D_{51}+D_{15}]\right\} \qquad (17)$$
$$+ \frac{9}{4}\left(\frac{\Gamma}{4}\right)^4\left\{D_{11} - 2[D_{31}+D_{13}] + [D_{51}+D_{15}] + 4D_{33} - 2[D_{53}+D_{35}] + D_{55}\right\} .$$

The collimating part still has to be treated numerically, of course. The results from the computations will be treated in a form corresponding to eq. (11):

$$|\rho_-| = \frac{\Lambda+2}{4}\,\rho_o a k_-\, M_a M_b\, F(y,\Gamma) , \qquad (18)$$

Where $F(y,\Gamma)$ is the modified form of $F(y)$ of eq. (11), the latter now corresponding to $F(y,0)$.

Fig. 2 shows a plot of $F(y,\Gamma)$ and $E(y,\Gamma)$ for three

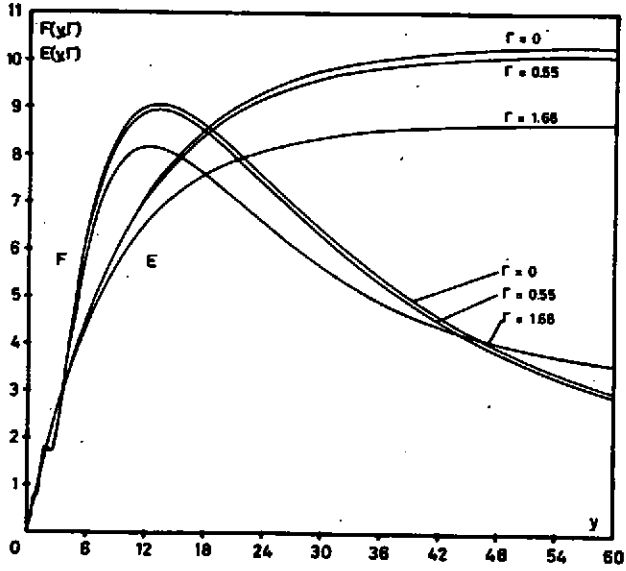

Fig. 2. Computed axial distribution for different primary amplitudes Γ. E refers to the infinite plane wave solution, F to the complete solution. Γ = 0.55 corresponds to Re = 0.08 when Λ = 5.

different values of Γ. The effect of a finite value of Γ is easily seen. The fact that the collimated distribution for Γ = 1.66 exceeds that of Γ = 0 for great distances is somewhat alarming, since the effect of nonlinear attenuation is to shorten the virtual array, which means that the amplitude should decay more rapidly along the axis. This argument is also supported by observations in the far field. The reason lies most probably in a small, yet undetected numerical error which is accumulative, since the curves fit well for small distances. Note that although Γ=1.66 gives L≈12a, so that eq.(15) becomes less accurate outside the maximum, this may hardly explain the effect just discussed.

For this reason we shall concentrate in the following only on the variations of the maximum with the primary amplitude. Fig.3 shows the observed and the computed

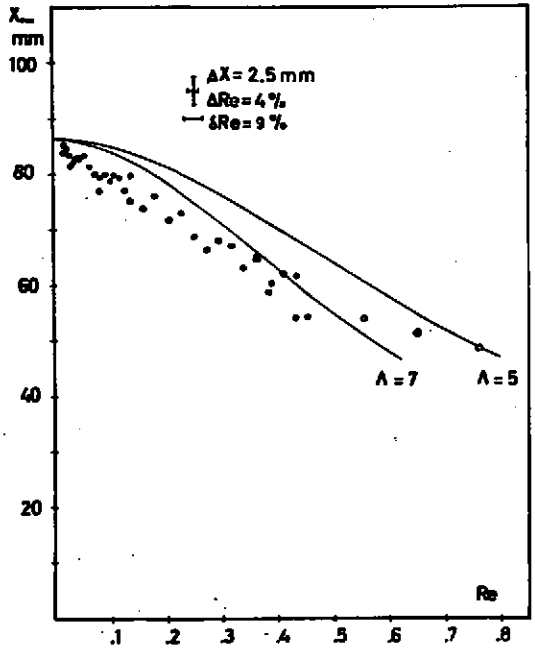

Fig.3. Observed and computed variation of x_{max} with primary amplitude. δ = systematic-, Δ = resolutional-uncertainities. When stated in % the bars shown are only of typical lengths.

variation of the distance to the maximum, x_{max}, with the primary amplitudes. The abscissa here is in Re, and although the best confirmed value of Λ for water is around 5, we decided to use it as a parameter, with the values 5 and 7 to cover the most probable values. The ordinate is x_{max} in mm. The uncertainities connected with the experimental values will be discussed in the next section. Although correspondence between the theoretical and the observed variation of x_{max} is not complete, it may be claimed to be satisfactory.

The variation of the amplitude with Γ is presented in fig.4, which shows $F(y_{max},\Gamma)/F(y_{max},0)$ versus Γ, together with the observed variation in terms of $(V_{obs}/V_aV_b)/(V_{obs}/V_aV_b)_{ref}$, with $\Lambda = 5$. Here V_a, V_b denote the voltages at the source transducer and V_{obs} the probe voltage. Thus only calibration of the source was necessary, namely to relate the observed points to Γ. $(V_{obs}/V_aV_b)_{ref}$ was chosen somewhat arbitrarily to ensure a proper normalization. Also here a satisfactory correspondence between theory and experiment has been obtained.

A comparison involving absolute values of amplitudes is shown in fig.5. This is a plot of the observed pressure as $P_{observed}/P_{calculated}$ versus Γ, for the values $\Lambda = 5$ and $\Lambda = 7$. Quite large uncertainities are involved, the systematic arising from calibration, and the scattering uncertainities from the equipment resolution. Nevertheless, for $\Lambda = 5$ correspondence is quite good. For $\Gamma > 2$ there is a trend towards higher observed values. This might be due to the effect of higher order interactions (see also discussion in Ref.(10)), but one should be aware also that for these primary amplitudes the discontinuity distance L will be shorter than x_{max} in this experiment, so that eq.(15) will become less applicable. Still similar trends may be seen, however, in the observations presented in fig.3, where for $Re > 0.4$ ($\Gamma > 2.8$) the x_{max} values seems to be somewhat less affected by an increase in the primary amplitude, than below $Re \approx 0.3$.

Thus it may be concluded that the effect of non-linear attenuation of the primary waves may account rather well for the observed changes in the axial maximum of the generated difference frequency sound, even in this rather crude way of compensating for the energy transfer to the second order waves.

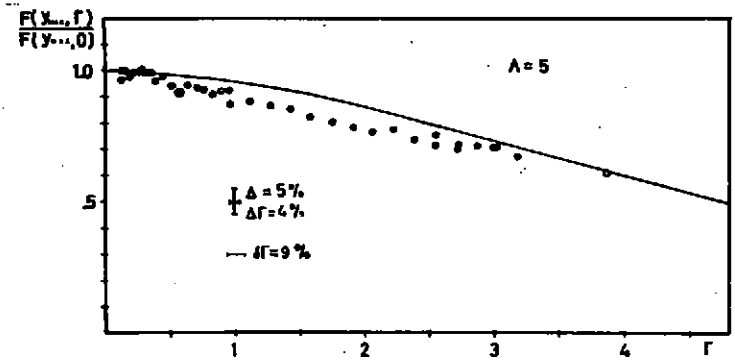

Fig. 4. The observed and computed relative change in maximum amplitude versus Γ.

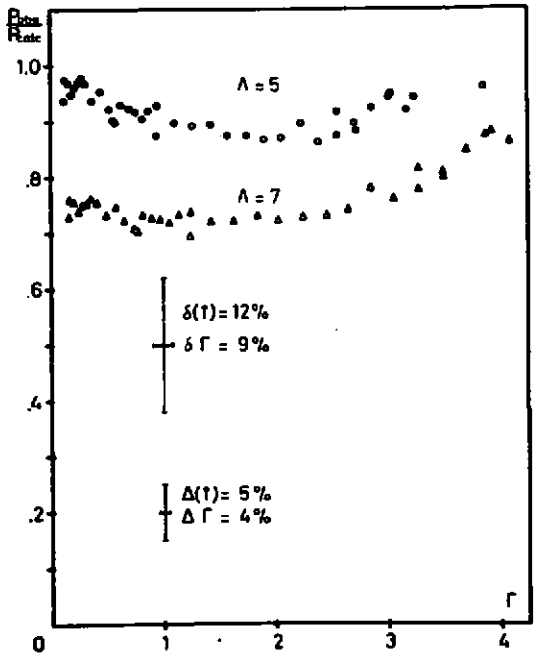

Fig. 5. Comparisons of observed and computed absolute pressure amplitude at the maximum versus Γ.

VI. The experiment.

The experimental configuration was as described in Ref.(1); only minor details have been subject to refinements. Continous waves were used throughout. Calibration of the source and the probe circuit was obtained by the use of a very sensitive radiometer, employing the method of Borgnis[14], and for the primary source the results have been given in terms of an effective electrical resistance R at the terminal where the primary voltages are measured. By employing the same RF-meter throughout, the calibration constant of this meter was eliminated from the measurements. All effects known to be involved by the use of radiometer measurements have been taken into account to reduce systematic errors. Although reproducibility indicates a spread of 2% in the obtained values of R we use a value of 5% for the largest possible error. This corresponds to an uncertainity of 7% in the intensity when uncertainities in the effective source radius (3%) and the voltage measurements (3%) are included.

From the calibration curve thus obtained two frequencies 1.0 MHz apart with equal R's were selected, and the primary frequencies 17.68 and 16.68 MHz were chosen, with $R = 53 \pm 2.5\ \Omega$. The same calibration procedure was used to calibrate a 1.0 MHz source, which then was used to calibrate the probe circuit. For the latter, one obtained the calibration constant

$$b = 535 \pm 10\%\ (N/m^2)/V \quad .$$

Of the other quantities involved, greatest uncertainity is connected with the attenuation coefficient β in $\alpha = \beta f^2$, where we have used $\beta = 2.5 \pm 0.2 \cdot 10^{-14} s^2/m$. Further we have used the values $a = 6.5 \pm 0.2 \cdot 10^{-3} m$, $c_o = 1.49 \cdot 10^3 m/s$ and $\rho_o = 10^3\ kg/m^3$. To obtain a proper comparison with theory only observed values where $\Gamma_a \approx \Gamma_b$ have been used. Since both systematic errors (δ), which will be constant, and resolutional errors (Δ), which will produce a spread in the observations, are very important in these comparisons, some discussion of the methods employed is necessary. What we observe is

$$P_{obs} = b\ V_{obs} = b\ V_a V_b\ H(y, V_a V_b) \qquad (19)$$

where H represents the distribution, while the calculated

pressure is

$$P_{calc} = c_o^2|\rho_-| = K_I M_a M_b F(y,\Gamma). \qquad (20)$$

To compare the distributions F and H one needs a relation between Γ (or Re) and V_aV_b. This may be expressed as

$$Re^2 = Re_a Re_b = \frac{2}{a^2\rho_o c_o^5 \beta^2} \frac{1}{f_a f_b \sqrt{R_a R_b}} V_a V_b = K_R V_a V_b . \qquad (21)$$

In our experiment we have $K_R = 1/482 \pm 13\%$, where the uncertainity is systematic and comes from $\delta\beta$ and $\delta(R_aR_b)$ chiefly. The Mach-numbers are related to the voltages by

$$M_a M_b = 2/(\pi a^2 \rho_o c_o^3 \sqrt{R_a R_b})\ V_a V_b . \qquad (22)$$

Comments fo fig.1.

Since we used continous waves it was impossible to eliminate completely the fluctuations which arise because of reflections in the tank. The most serious fluctuations turned out to originate from the suspension system of the probe, and when these were reduced by the aid of a sharp-edged V-reflector, the fine structure near the source (the "hump") became easily detectable. Small fluctuations still exist, however, and the distribution shown in fig.1 is a smoothed version of the really observed distribution.

Comments to fig.3.

The observed x_{max} are obtained from observed distributions similar to fig.1. Uncertainities in x_{max} come from resolution and are not systematic: $\Delta x_{max} = 2.5$ mm. Uncertainities in Re are partly systematic (δK_R): $\delta Re = 9\%$, partly resolutional (ΔV): $\Delta Re = 4\%$.

Comments to fig.4.

We want to plot $H(y_{max}, V_aV_b)/H(y_{max}, 0)$ versus Γ. From eq.(19) one has

$$H(y_{max}, V_aV_b)/H(y_{max},0) = \left\{(V_{obs}/V_aV_b)/(V_{obs}/V_aV_b)_{ref}\right\}_{y_{max}}$$

where $(V_{obs}/V_aV_b)_{ref} = \lim_{V\to 0}\left\{V_{obs}/V_aV_b\right\}$. Vertically one has a possible systematic error from the choice of the reference value, which is ignored. There remains then a resolutional uncertainity Δ of order 5% arising from ΔV. Horizontally we still have $\delta\Gamma = 9\%$ and $\Delta\Gamma = 4\%$.

Comments to fig.5.

From eq.(19) and eq.(20) one obtains

$$\frac{P_{obs}}{P_{calc}} = \frac{b\,V_{obs}}{K_I M_a M_b F(y,\Gamma)} = K_{II}\,\frac{V_{obs}}{V_a V_b}\,\frac{1}{F(y,\Gamma(V_a V_b))}$$

where $K_{II} = bac_o^2\sqrt{R_a R_b}\,/(A+2)f_-$. Note that A enters K_{II}. Only systematic errors are present in K_{II}, arising from δb and δR chiefly. Systematic errors also come from F because of $\Gamma(V_a V_b)$, but it is easily seen from fig.4 that an error of 9% in Γ gives at most an error of 3% in F. This gives us a possible systematic error $\delta(P_{obs}/P_{calc}) = 12\%$ and a resolutional error $\Delta(P_{obs}/P_{calc}) = 5\%$, while we still have $\delta\Gamma = 9\%$ and $\Delta\Gamma = 4\%$ along the horizontal axis.

VII. Discussions.

Evidently, as long as attenuation terminates interaction before the primary waves reach their far field, the assumption of plane collimated primary waves seems to be adequate to describe the axial distribution of the generated difference frequency sound. As apparent from eq.(9) the difference frequency sound may be thought of as beeing radiated from an array of circular piston sources with radius the same as the primary source, and spatially tapered in amplitude like the product of the primary waves. If the array length is made infinitesimal the resulting field would be the same as that of an ordinary piston source of the same frequency and radius (hereafter referred to as OPS). The effect of a finite length of the array should then be to smooth the field, so that diffraction fluctuations should become smaller than those from an OPS. Still, even in an array of infinite length (primary beam plane, though) remnants of the diffraction fluctuations should be present in the vicinity of the primary source, superposed on the dominant part of the field, which will be linearly increasing with distance. In this case no true axial maximum will exist, of course. The latter appears to be due to a combination of the effects of diffraction, the finite length of the array and attenuation of the generated wave (when important). If the latter is negligible it is easy to see that the axial maximum ("diffraction maximum") will be situated outside the last axial maximum of the OPS, and coincide with the

latter only when the array is infinitesimal in length. This will not necessarily be the case when the attenuation of the generated wave is of importance, however, and if in addition the array length is much shorter than the length of the OPS near field, one should expect diffraction effects to be negligible and the maximum to behave as an "attenuation maximum", as in the infinite plane wave case.

The same arguments should apply to the second harmonics and the sum frequency waves. Here, however, the "diffraction maximum" should occur outside the near field of the primary waves, so that to describe it properly the more complicated properties of the primary near fields must be taken into account (especially the paraxial region). Roughly, since the primary waves diverge in their far field, one should expect this to shift the "diffraction maximum" inwards and place it somewhere near the last axial maximum of the primary waves. Still, the plane collimated wave model should apply when attenuation is high enough, so that the waves will experience an "attenuation maximum" instead of a "diffraction maximum".

Concerning our assumption in Section V, that these waves behave like plane waves, we should be on safe ground, since until a "diffraction maximum" is reached the waves should be very nearly plane inside the beam. Since the latter maximum should occur near the limit of the near field of the primary waves, the initial condition, i.e. termination of interaction inside the primary near field, will ensure plane high frequency second order waves within the interaction region. This is also confirmed by the observations of Gould et al. (op.cit.) which show that the second harmonic is well collimated even at a distance twice the distance to the "diffraction maximum".

Depletion of the primary waves due to generation of second harmonics and sum frequency waves seems to be sufficient to account for the observed variations of the axial maximum of the generated difference frequency sound. Provided $\Gamma < 1$ or $x < L$, eq. (15) should be adequate to account for this depletion of the primary waves. For higher amplitudes and $x > L$ this equation will no longer be appropriate, however, a property which it shares with the third order approximation of Burgers equation, since at this level the effect of higher order waves can no

longer be neglected[10]. Still, the results presented here show that when the maximum is concerned the deviations between theory and observations are quite small even for large primary amplitudes. At great distances from the primary source, however, it is to be expected that the limitations of eq.(15) will be much more pronounced.

References.

1 H. Hobæk, J. Sound Vibration 6, 460-463 (1967).
2 V.A. Zverev and A.I. Kalachev, Soviet Phys. Acoust. 14, 173-178 (1968).
3 K. Brinkmann, Acustica 20, 92-100 (1968).
4 T.G. Muir and J.E. Blue, J. Acoust. Soc. Amer. 46, 227-232 (1969).
5 K.A. Nagol'nykh, S.I. Soluyan and R.V. Khokhlov, Soviet Phys. Acoust. 9, 155-159 (1963).
6 V. Lauvstad, J. Naze and S. Tjøtta, Årbok Univ. Bergen, Mat.-Nat. Ser. No 12 (1964).
7 H. Hobæk, Scientific/Technical Report no 32, Dep. of Physics, Univ. Bergen (1970).
8 R.K. Gould, C.W. Smith, A.O. Williams Jr. and R.P. Ryan, J. Acoust. Soc. Amer. 40, 421-427 (1966).
9 S. Tjøtta, J. Sound Vibration 6, 255-267 (1967).
10 O.M. Faltinsen and S. Tjøtta, Paper presented at this meeting.
11 J.M. Manley and H.E. Rowe, Proc. Inst. Radio Engrs. 44, 904 (1956).
12 W. Keck and R.T. Beyer, Phys. Fluids 3, 346-352 (1960).
13 D.T. Blackstock, J. Acoust. Soc. Amer. 39, 411-413 (1966).
14 F.E. Borgnis, J. Acoust. Soc. Amer. 25, 546-548 (1953).

† This equation was originally presented erroneously with a factor 4 instead of 3 in the last term. The correction of this error turned out to be of little consequence and did not change any of the conclusions drawn from the earlier results. Still, the results presented here are computed from the corrected equation.

Appendix. The near field of a circular piston source.

The results from Ref.(7) may be summarized as follows:

1. The near field has the overall structure of a beam, beeing well defined near the source, but diffusing more and more with distance. From the beam there is a continous radiation of sidelobes, the amplitudes of which increase with the distance from where they emerge from the beam. The total number of sidelobes is $2N-\frac{1}{4}$, including the main lobe which dominates the beam for $Z > 1$.
2. Inside the beam the field consists of a superposition of those lobes which have not yet emerged. The structure of the field is accordingly very complicated, but may roughly be classified as a "plateau" of amplitude equal to 1 (in dimensionless pressure), on which are superposed a set of large and a set of small fluctuations. With increasing distance from the source the larger fluctuations tend to move toward the axis, while the smaller fluctuations always move outwards, and show individual existance as sidelobes outside the beam. This is of course also the destiny of the larger fluctuations, but only after having crossed the axis.
3. The gross structure of the beam is determined by the large fluctuations. The amplitudes of these are greatest at the axis, where they may cancel the plateau, but decay rapidly outside the paraxial region. At the beam edge, however, there is a slight increase in the amplitudes again, and the last maximum has an amplitude of ca. 0.2 above the plateau. This amplitude is almost constant for $Z < 0.5$. The latter maximum finally reaches the axis as a sole survivor, and composes the main lobe. The number of large fluctuations at any distance from the source may easily be calculated from

$$n = [(x^2+a^2)^{\frac{1}{2}} - x]/\lambda \approx 1/2Z \text{ when } Z > 1/N. \quad (A1)$$

4. At $b = 1$ the amplitude of the field is always close to 0.5 for $Z < 1$. The beam itself, defined for instance by the lateral extension of the plateau, appears to contract slightly with increasing Z, although this contraction is poorly defined as the beam edge becomes more and more diffuse.

5. The phase angle fluctuates very little across the beam. For $b \leq 1$ it is centered at the same value as that of an infinite plane wave of same wavelength and initial conditions. For $b > 1$ the phase angle recedes rapidly. Inside the beam the phase fluctuations on a cross section are typically of order 20 degrees, except within the paraxial region where they may be some 3-4 times greater near the source. With increasing distance the magnitude of these fluctuation decreases, however, so that one for most practical purposes may assume that the phase angle is constant across the beam.
6. When linear attenuation is included attenuation takes place almost as for a plane wave. Very little relative change may be detected in the structure of the field, and the phase angles behave as in the ideal case.

As an illustration to these conclusions figs. A1-A3 show cross sections of the computed field of the source used in our experiments at distances 10, 50 and 90 mm from the source. Here $N = 76.4$ ($ka = 480$) corresponding to $f = 17.68$ MHz in water. The horizontal axis is lateral distance from the axis in mm. The upper curves show phase angles in degrees (right vertical axis) while the lower curves show the dimensionless pressure amplitude (left vertical axis). Also included are the amplitude and phase of a plane collimated wave of the same frequency and initial phase. Attenuation is neglected. n refers to the value obtained from eq. (A1).

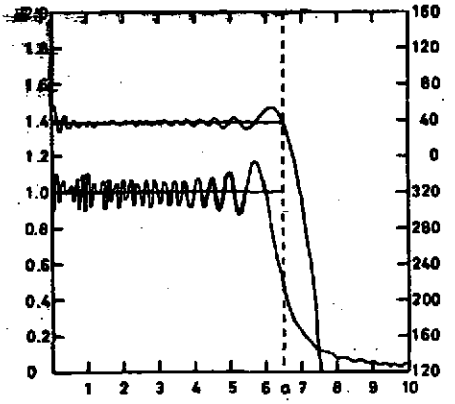

Fig. A1.
x = 10 mm,
Z = 0.02,
n = 22.67 .

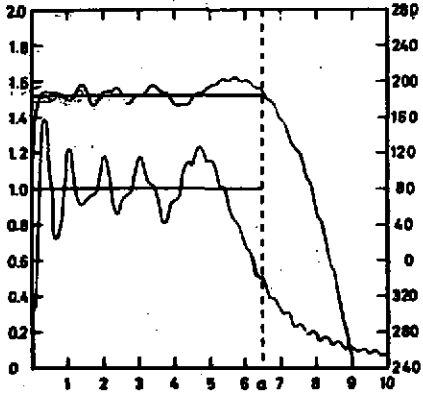

Fig. A2.
x = 50 mm,
Z = 0.1006,
n = 4.95 .

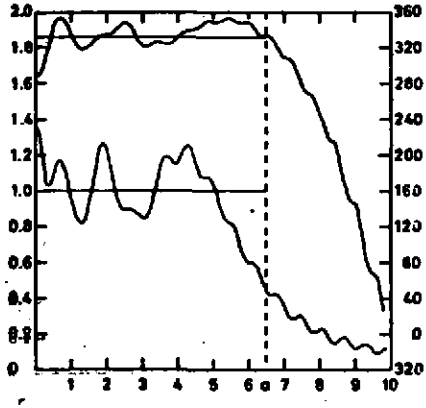

Fig. A3.
x = 90 mm,
Z = 0.18106,
n = 2.76 .